

Controlling the Rotational and Hyperfine State of Ultracold $^{87}\text{Rb}^{133}\text{Cs}$ Molecules

Philip D. Gregory,¹ Jesus Aldegunde,² Jeremy M. Hutson,^{3,*} and Simon L. Cornish^{1,†}

¹*Joint Quantum Centre (JQC) Durham-Newcastle, Department of Physics,
Durham University, South Road, Durham DH1 3LE, United Kingdom*

²*Departamento de Química Física, Universidad de Salamanca, 37008 Salamanca, Spain*

³*Joint Quantum Centre (JQC) Durham-Newcastle, Department of Chemistry,
Durham University, South Road, Durham, DH1 3LE, United Kingdom*

We demonstrate coherent control of both the rotational and hyperfine state of ultracold, chemically stable $^{87}\text{Rb}^{133}\text{Cs}$ molecules with external microwave fields. We create a sample of ~ 2000 molecules in the lowest hyperfine level of the rovibronic ground state $N = 0$. We measure the transition frequencies to 8 different hyperfine levels of the $N = 1$ state at two magnetic fields ~ 23 G apart. We determine accurate values of rotational and hyperfine coupling constants that agree well with previous calculations. We observe Rabi oscillations on each transition, allowing complete population transfer to a selected hyperfine level of $N = 1$. Subsequent application of a second microwave pulse allows transfer of molecules back to a different hyperfine level of $N = 0$.

Ultracold heteronuclear molecules can provide many exciting new avenues of research in the fields of quantum state controlled chemistry [1, 2], quantum information [3], quantum simulation [4, 5], and precision measurement [6–8]. The large electric dipole moments accessible in such systems allow interactions to be tuned over length scales similar to the spacing between sites in an optical lattice. As such, this is an area of intense research with multiple groups recently reporting the production of dipolar molecules at ultracold temperatures [9–13].

Full control of the quantum state has been an invaluable tool in ultracold atom physics; it is therefore highly important to develop similar methods for ultracold molecules which address the complex rotational and hyperfine structure. Such control is at the heart of nearly all proposals for applications of ultracold polar molecules. For example, the rotational states of molecules might be used as pseudo-spins to simulate quantum magnetism [14, 15]. This requires a coherent superposition of opposite-parity states to generate dipolar interactions [14], which may be probed by microwave spectroscopy [16, 17]. Similarly, hyperfine states in the rotational ground state have been proposed as potential qubits for quantum computation [3, 18, 19]. In this context, robust coherent transfer between the hyperfine states is essential. Such transfer can be achieved using a scheme proposed by Aldegunde *et al.* [20] which employs microwave fields to manipulate the molecular hyperfine states. This approach has been implemented for the fermionic heteronuclear molecules $^{40}\text{K}^{87}\text{Rb}$ [21, 22] and $^{23}\text{Na}^{40}\text{K}$ [23], leading to ground-breaking studies of the dipolar spin-exchange interaction [17] and nuclear spin coherence time [19].

In this letter, we report microwave spectroscopy of bosonic $^{87}\text{Rb}^{133}\text{Cs}$ in its ground vibrational state, and coherent state transfer from the absolute rovibrational

and hyperfine ground state to a chosen well-defined single hyperfine state in either the first-excited or ground rotational states. We demonstrate the high precision with which we can map out the rotational energy structure of the $^{87}\text{Rb}^{133}\text{Cs}$ molecule in the lowest vibrational state. We use our measurements to obtain new values for the rotational constant, scalar spin-spin coupling constant, electric quadrupole coupling constants, and nuclear g -factors (including shielding) for the molecule. Microwave π -pulses are used to transfer the molecules first to a single hyperfine level of the first-excited rotational state, then back to a different hyperfine level of the rovibrational ground state.

We calculate the energy level structure of $^{87}\text{Rb}^{133}\text{Cs}$ in the electronic and vibrational ground state by diagonalizing the relevant Hamiltonian. In the presence of an externally applied magnetic field, this Hamiltonian (H) can be decomposed into rotational (H_r), hyperfine (H_{hf}), and Zeeman (H_Z) components [24–27]

$$H = H_r + H_{\text{hf}} + H_Z. \quad (1)$$

These contributions are given by

$$H_r = B_v N^2 - D_v N^2 N^2, \quad (2a)$$

$$H_{\text{hf}} = \sum_{i=\text{Rb,Cs}} \mathbf{V}_i \cdot \mathbf{Q}_i + \sum_{i=\text{Rb,Cs}} c_i \mathbf{N} \cdot \mathbf{I}_i + c_3 \mathbf{I}_{\text{Rb}} \cdot \mathbf{T} \cdot \mathbf{I}_{\text{Cs}} + c_4 \mathbf{I}_{\text{Rb}} \cdot \mathbf{I}_{\text{Cs}}, \quad (2b)$$

$$H_Z = -g_r \mu_N \mathbf{N} \cdot \mathbf{B} - \sum_{i=\text{Rb,Cs}} g_i (1 - \sigma_i) \mu_N \mathbf{I}_i \cdot \mathbf{B}. \quad (2c)$$

The rotational contribution (Eqn. 2a) is defined by the rotational angular momentum of the molecule \mathbf{N} , and the rotational and centrifugal distortion constants B_v and D_v . The hyperfine contribution (Eqn. 2b) consists of four terms. The first term describes the electric quadrupole interaction with coupling constants $(eqQ)_{\text{Rb}}$ and $(eqQ)_{\text{Cs}}$. The second term is the interaction between the nuclear magnetic moments and the magnetic field generated by the rotation of the molecule, with spin-rotation coupling constants c_{Rb} and c_{Cs} . The final two

* J.M.Hutson@durham.ac.uk

† S.L.Cornish@durham.ac.uk

terms represent the tensor and scalar interactions between the nuclear magnetic moments, with tensor and scalar spin-spin coupling constants c_3 and c_4 respectively. Finally, the Zeeman contribution (Eqn. 2c) consists of two terms which represent the rotational and nuclear interaction with an externally applied magnetic field. The rotation of the molecule produces a magnetic moment which is characterized by the rotational g -factor of the molecule (g_r). The nuclear interaction similarly depends on the nuclear g -factors (g_{Rb} , g_{Cs}) and nuclear shielding (σ_{Rb} , σ_{Cs}) for each species. We do not apply electric fields in this work, which would require the addition of a further Stark contribution to the Hamiltonian and significantly complicate the spectra [28].

The nuclear spins in $^{87}\text{Rb}^{133}\text{Cs}$ are $I_{\text{Rb}} = 3/2$ and $I_{\text{Cs}} = 7/2$. At zero field, the total angular momentum $\mathbf{F} = \mathbf{N} + \mathbf{I}_{\text{Rb}} + \mathbf{I}_{\text{Cs}}$ is conserved. For the rotational ground state ($N = 0$), the total nuclear spin $\mathbf{I} = \mathbf{I}_{\text{Rb}} + \mathbf{I}_{\text{Cs}}$ is very nearly conserved, and there are 4 hyperfine states with $I = 2, 3, 4$ and 5 with separations determined by c_4 [27]. For excited rotational states, however, only F is conserved and I is a poor quantum number.

An external magnetic field splits each rotational manifold into $(2N+1)(2I_{\text{Rb}}+1)(2I_{\text{Cs}}+1)$ Zeeman-hyperfine sublevels, so there are 32 levels for $N = 0$ and 96 levels for $N = 1$. Assignment of quantum numbers to the individual hyperfine levels is non-trivial and depends on the magnetic field regime [27]. The field mixes states with different values of F that share the same total projection M_F . At low field, the levels are still approximately described by F and M_F (equivalent to I and M_I for $N = 0$). At high field, however, the nuclear spins decouple and the individual projections M_N , m_I^{Rb} and m_I^{Cs} become nearly good quantum numbers, with $M_F = M_N + m_I^{\text{Rb}} + m_I^{\text{Cs}}$.

A microwave field induces electric dipole transitions between rotational levels. At low field, all transitions allowed by the selection rules $\Delta F = 0, \pm 1$ and $\Delta M_F = 0, \pm 1$ have significant intensity. At higher field, however, additional selection rules emerge. If hyperfine couplings are neglected, electric dipole transitions leave the nuclear spin states unchanged ($\Delta m_I^{\text{Rb}} = \Delta m_I^{\text{Cs}} = 0$) and are allowed only between neighboring rotational states such that $\Delta N = \pm 1$, $\Delta M_N = 0, \pm 1$ for microwave polarizations π, σ^\pm . In the absence of hyperfine interactions (where M_N would be a good quantum number) we would be able to drive at most three transitions from any given hyperfine level, as shown in Fig. 1(a). Nuclear quadrupole coupling in the $N = 1$ state mixes levels with different values of M_N , m_I^{Rb} and m_I^{Cs} , and additional transitions become allowed. The relative strengths of the transitions depend on the magnitude of the component of the destination state that preserves m_I^{Rb} and m_I^{Cs} [20]. The presence of state mixing allows us to use a multi-photon scheme to move the population to different hyperfine states of the rotational ground state. Fig. 1(b) shows an example of the simplest possible variation of the scheme using two microwave photons to change the hyperfine state by $\Delta M_F = -1$.

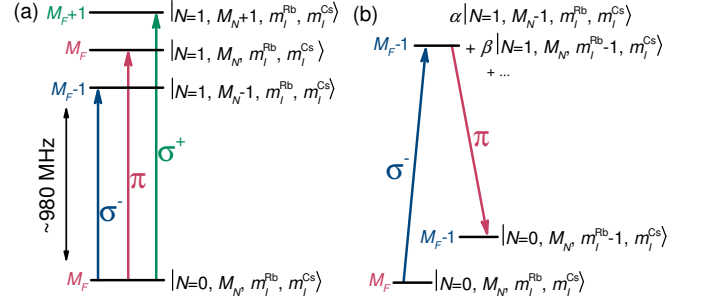


FIG. 1. (Color online) Electric dipole transitions in $^{87}\text{Rb}^{133}\text{Cs}$ between the $N = 0$ and $N = 1$ rotational levels in the vibrational ground state. (a) First-order allowed electric-dipole transitions keep the hyperfine state projections from the atomic nuclear angular momentum unchanged ($\Delta m_I^{\text{Rb}} = \Delta m_I^{\text{Cs}} = 0$). In the absence of hyperfine interactions we would therefore expect to be able to drive 3 transitions with $\Delta M_F = \Delta M_N = 0, \pm 1$ for microwave polarizations π, σ^\pm . (b) Scheme for changing nuclear angular momentum in the rotational ground state. Interactions involving the nuclear electric quadrupole moments of ^{87}Rb and ^{133}Cs mix quantum states with different nuclear spin quantum numbers m_I^{Rb} and m_I^{Cs} . We use a two-photon pulse sequence to transfer up to a mixed excited quantum state in which both the initial and desired values of M_N are present.

Our experimental apparatus and method for creating ultracold $^{87}\text{Rb}^{133}\text{Cs}$ molecules have been discussed in previous publications [11, 29–34]; we will therefore give only a brief overview here. We begin by using magnetoassociation on a magnetic Feshbach resonance to create weakly bound molecules from an ultracold atomic mixture confined in a crossed-beam optical trap ($\lambda = 1550$ nm) [33]. We remove the remaining atoms by means of the Stern-Gerlach effect, leaving a pure sample of trapped molecules. These molecules are then transferred to a single hyperfine state of the rovibrational ground-state by stimulated Raman adiabatic passage (STIRAP) [11, 35]. In this work, we create a sample of up to ~ 2000 $^{87}\text{Rb}^{133}\text{Cs}$ molecules in the lowest hyperfine state (shown in Fig. 2(a)) at a temperature of $1.17(1) \mu\text{K}$ and peak density of $8.1(8) \times 10^{10} \text{ cm}^{-3}$. It is important to note that in order to measure the number of molecules in our experiment we reverse both the STIRAP and magnetoassociation steps and subsequently use absorption imaging to detect the atoms that result from the molecular dissociation. Throughout, therefore, we always measure the number of molecules in the hyperfine state initially populated by STIRAP.

Our apparatus is equipped with two omnidirectional $\lambda/4$ antennas placed close to the outside of the fused silica cell. The polarization from each is roughly linear at the position of the molecules. They are oriented perpendicular to each other and aligned with respect to the direction of the static magnetic field such that one preferentially drives transitions with $\Delta M_F = 0$ and the other drives those with $\Delta M_F = \pm 1$. Each antenna is con-

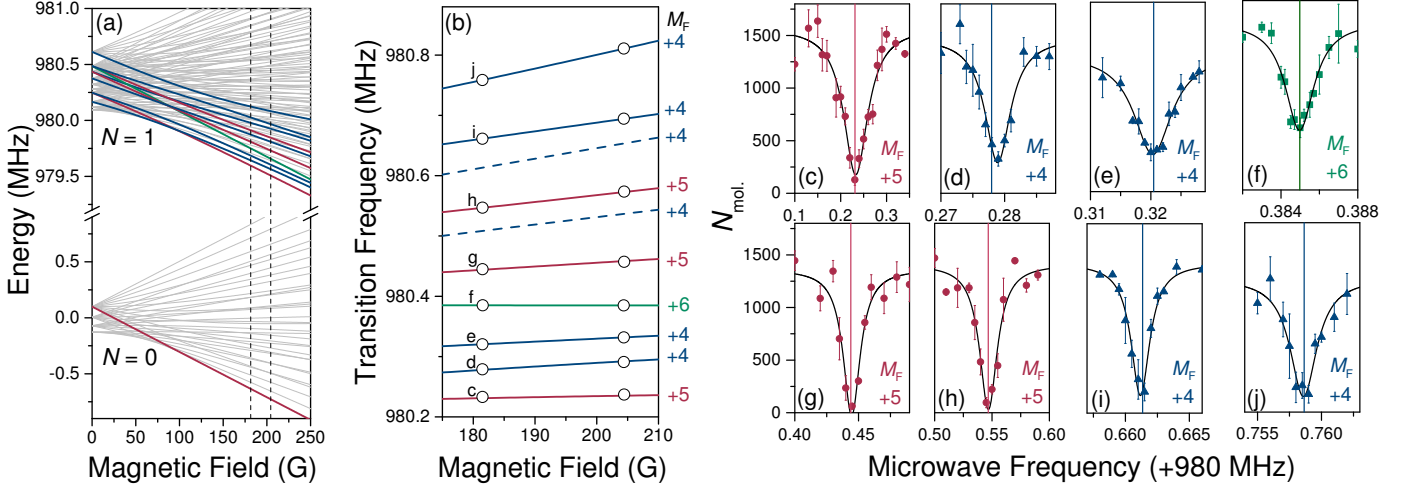


FIG. 2. (Color online) Spectroscopy of the first-excited rotational state. (a) Hyperfine Zeeman structure of the $N = 0$ and $N = 1$ states. The initial state in $N = 0$ is highlighted as the bold red line. The 10 states that are accessible from this initial state in $N = 1$ are shown as bold blue ($M_F = 4$), red ($M_F = 5$), and green ($M_F = 6$) lines. The vertical dotted lines mark the two magnetic fields at which spectroscopy is performed in this work. (b) Comparison of experimentally measured transition frequencies from $|N = 0, M_F = 5\rangle$ to $|N = 1, M_F = 4, 5, 6\rangle$ with the fitted theory. Dashed lines indicate transitions that are weakly allowed but we have not observed. Error bars are not visible at this scale (see Table I). (c-j) Spectra of all the transitions found in this work at a magnetic field of ~ 181.5 G. The vertical lines shows the position of each transition given by fit to the results. The widths of all of the features are Fourier-transform limited. The pulse duration used is less than a π pulse for each transition. The specific pulse durations are (c) 12 μs , (d) 150 μs , (e) 100 μs , (f) 400 μs , (g) 60 μs , (h) 50 μs , (i) 400 μs , (j) 200 μs .

M_F	B (G)	$f_{\text{The.}}$ (kHz)	$f_{\text{Exp.}}$ (kHz)	Δf (kHz)
+5	181.507(2)	980 231.07	980 233(2)	-2(2)
	204.436(2)	980 235.14	980 237(1)	-2(1)
+4	181.484(1)	980 277.96	980 278.9(2)	-0.9(2)
	204.397(2)	980 292.08	980 291.0(2)	1.1(2)
+4	181.487(1)	980 320.47	980 320.4(2)	0.1(2)
	204.397(2)	980 331.83	980 331.8(3)	0.0(3)
+6	181.541(2)	980 384.98	980 384.97(6)	0.01(6)
	204.38(1)	980 384.87	980 384.90(5)	-0.03(5)
+5	181.507(2)	980 443.97	980 444.8(7)	-0.8(7)
	204.436(2)	980 458.35	980 457.2(8)	1.1(3)
+5	181.507(2)	980 546.75	980 546.9(7)	-0.2(7)
	204.436(2)	980 572.86	980 573.5(6)	-0.6(6)
+4	181.487(1)	980 661.35	980 661.15(6)	0.20(6)
	204.397(2)	980 694.22	980 694.35(5)	-0.13(5)
+4	181.487(1)	980 758.64	980 758.6(1)	0.0(1)
	204.397(2)	980 810.62	980 810.8(3)	-0.2(3)

TABLE I. Microwave transitions found in $^{87}\text{Rb}^{133}\text{Cs}$ from $|v = 0, N = 0\rangle$ to $|v = 0, N = 1\rangle$. All transitions start from the spin-stretched $M_F = +5$ hyperfine level of the rotational ground state. Each transition is labeled by the M_F quantum number of the destination hyperfine level in the first-excited rotational state.

connected to a separate signal generator, which is frequency referenced to an external 10 MHz GPS reference. Fast ($\sim\text{ns}$) switches are used to generate microwave pulses of well-defined duration (typically 1 μs - 500 μs).

The large dipole moment of the molecule (1.225 D [11]) makes it easy to drive fast Rabi oscillations between neighboring rotational states. To perform the spec-

troscopy, therefore, we pulse on the microwave field for a time (t_{pulse}) which is less than the duration of a π -pulse for the relevant transition ($< t_{\pi}$). We then observe the transition as an apparent loss of molecules as they are transferred into the first-excited rotational state. To avoid ac Stark shifts of the transition centers, the optical trap is switched off throughout the spectroscopy; the transition frequencies are thus measured in free space. We find that the widths of all of the features we measure are Fourier-transform limited, i.e. the width is proportional to $1/t_{\text{pulse}}$. We therefore iteratively reduce the power to get slower Rabi oscillations and allow longer pulse durations. We also note that radically different t_{pulse} are required for each transition depending on the transition strength and antenna used. We carry out the spectroscopy at two different magnetic fields ~ 23 G apart; the magnetic field is calibrated using the microwave transition frequency between the $|f = 3, m_f = +3\rangle$ and $|f = 4, m_f = +4\rangle$ states of Cs.

With the population initially in the lowest hyperfine level ($M_F = 5$) of the rovibrational ground state, we expect to find a maximum of 10 transitions to the first-excited rotational state $|N = 1, M_F = 4, 5, 6\rangle$. We are able to observe 8 of these transitions, at the frequencies given in Table I. A complete set of spectra at a magnetic field of ~ 181.5 G is also shown in Fig. 2(c-j). Calculations of the expected intensities of the two unseen transitions show that the relative transition probability is $\sim 10^{-4}$ lower than for those we do observe.

We fit our model to the experimental spectra by minimizing the sum of the squared quotients between each residual and the uncertainty of the line. We fit the rotational constant, nuclear quadrupole constants and

Constant	Value	Ref.
B_v	490.155(5) MHz	[36]
D_v	490.173 994(45) MHz	This Work
$(eQq)_{\text{Rb}}$	213.0(3) Hz	[36]
$(eQq)_{\text{Cs}}$	-872 kHz	[27]
	-809.29(1.13) kHz	This Work
c_{Rb}	51 kHz	[27]
c_{Cs}	59.98(1.86) kHz	This Work
c_3	29.4 Hz	[27]
c_4	196.8 Hz	[27]
	192.4 Hz	[27]
	17.3 kHz	[27]
g_r	19.019(105) kHz	This Work
	0.0062	[27]
$g_{\text{Rb}} \cdot (1 - \sigma_{\text{Rb}})$	1.8295(24)	This Work
$g_{\text{Cs}} \cdot (1 - \sigma_{\text{Cs}})$	0.7331(12)	This Work

TABLE II. Constants involved in the molecular Hamiltonian for $^{87}\text{Rb}^{133}\text{Cs}$. Parameters not varied in the least-squares fit are taken from the literature. The majority of the fixed terms are calculated using density-functional theory (DFT) [27], with the exception of the centrifugal distortion constant D_v , which is obtained from laser-induced fluorescence combined with Fourier transform spectroscopy (LIF-FTS) [36]).

scalar nuclear spin-spin constant. The nuclear g -factors and shielding coefficients are multiplied together in the Hamiltonian so it is not possible to separate them, and we therefore fit the shielded g -factors $g_{\text{Rb}} \cdot (1 - \sigma_{\text{Rb}})$ and $g_{\text{Cs}} \cdot (1 - \sigma_{\text{Cs}})$. The resulting values, along with the values of parameters held fixed at theoretical values, are given in Table II.

The fitted hyperfine parameters in Table II are all within 10% of the values predicted from DFT calculations [27], except for $(eQq)_{\text{Cs}}$, which is about 15% larger than calculated. This helps to calibrate the probable accuracy of the calculations for other alkali-metal dimers. The fitted value $c_4 = 19.0(1)$ kHz removes one of the two largest sources of error in our recent determination of the binding energy D_0 of $^{87}\text{Rb}^{133}\text{Cs}$ in its rovibrational ground state [37]; the zero-field hyperfine energy of the $M_F = 5$ state is $(21/4)c_4$, which increases from 90(30) kHz in ref. [37] to 99.9(6) kHz. This increases the binding energy of the hyperfine-weighted vibronic bound state by 9 kHz, giving a revised value $D_0 = h \times 114\,268\,135.25(3)$ MHz. The fitted values of the shielded g -factors $g_{\text{Rb}} \cdot (1 - \sigma_{\text{Rb}}) = 1.829(2)$ and $g_{\text{Cs}} \cdot (1 - \sigma_{\text{Cs}}) = 0.733(1)$ are consistent with the corresponding atomic values, 1.827 232(2) [38] and 0.732 357(1) [39] (with the sign convention of Eqn. 2c). The latter include shielding due to the electrons in the free atoms. Our values may be used in conjunction with the calculated molecular shielding factors ($\sigma_{\text{Rb}} = 3531$ ppm and $\sigma_{\text{Cs}} = 6367$ ppm [27]) to obtain values of the “bare” nuclear g -factors 1.836(3) and 0.738(1).

The STIRAP transfer produces molecules in a spin-stretched state, where $|m_I^{\text{Rb}} + m_I^{\text{Cs}}|$ has its maximum possible value and $M_N, m_I^{\text{Rb}}, m_I^{\text{Cs}}$ are all good quan-

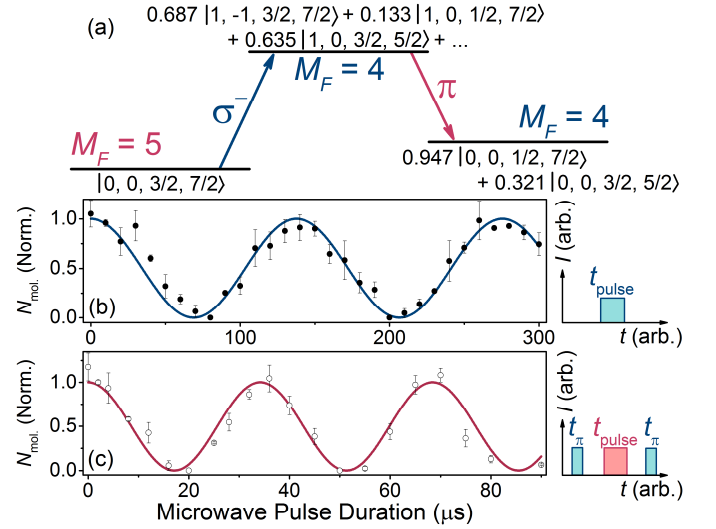


FIG. 3. (Color online) Coherent population transfer of molecules between hyperfine states in rotational states $N = 0$ and $N = 1$. (a) Transfer scheme followed in this work. All molecules start in the lowest hyperfine level ($M_F = 5$) of the rovibrational ground state. State notation is given by $|N, M_N, m_I^{\text{Rb}}, m_I^{\text{Cs}}\rangle$. (b) One-photon transfer of molecules to a single hyperfine level of the $N = 1$ excited rotational state. Microwaves with σ^- polarization drive transitions to $|N = 1, M_F = +4\rangle$. By varying the duration of the microwave pulse, we observe Rabi oscillations to determine the duration of a π -pulse allowing complete population transfer to the excited rotational state. (c) Two-photon transfer to change the hyperfine level populated in the rovibrational ground state. Once the population has been transferred to the $N = 1$ excited state, we introduce a second microwave pulse with different frequency and polarization from the first. This drives the population back down to a different hyperfine level of the rovibrational ground state than that initially populated.

tum numbers. However, the other hyperfine states of both $N = 0$ and 1 are significantly mixed in the uncoupled basis set at the fields considered here, and have no good quantum numbers other than M_F . In Fig. 3, we demonstrate complete transfer of the molecular population between these mixed-character hyperfine states. We begin by transferring the molecules to an $M_F = 4$ level of $N = 1$ (transition frequency = 980320.47 kHz, shown in Fig. 2(e)). The eigenvector component of the uncoupled basis function that couples to our initial $N = 0$ hyperfine level is ~ 0.687 . With the microwave power available, π -pulses on this transition can be driven with pulse durations $< 10 \mu\text{s}$, though it is important when using short pulses that the separation between available states is greater than the Fourier width of the pulse. We reduce the microwave power such that the Rabi frequency of the transition is $2\pi \times 7.26(5)$ kHz, as shown in Fig. 3(b), ensuring that we do not couple to neighboring transitions. Single π -pulses allow complete transfer of the population to the destination hyperfine level. We subsequently transfer the molecules to a different hyperfine level of $N = 0$ by applying a

second microwave field with a different polarization and frequency. We choose to use π -polarized microwaves to transfer the molecules to the higher-energy of the two $M_F = 4$ levels of $N = 0$ (transition frequency = 980119.14 kHz). At this field, the composition of this final level is $0.947 |4, 0, 1/2, 7/2\rangle + 0.321 |4, 0, 3/4, 5/2\rangle$ in the uncoupled basis $|N, M_N, m_I^{\text{Rb}}, m_I^{\text{Cs}}\rangle$. We observe Rabi oscillations on the second transition by pulsing on the π -polarized microwaves in between two π -pulses on the σ^- -polarized microwave transition as shown in Fig. 3(c). Coherent transfer is achieved with a Rabi frequency of $2\pi \times 29.2(3)$ kHz.

In summary, we have performed high-precision microwave spectroscopy of ultracold $^{87}\text{Rb}^{133}\text{Cs}$ molecules in the vibrational ground state, and have accurately determined the hyperfine coupling constants for the molecule. Our results confirm that the hyperfine coupling constants calculated by Aldegunde *et al.* [27] are generally accurate to within $\pm 10\%$, calibrating the probable accuracy of the calculations for other alkali-metal dimers. The resulting understanding of the hyperfine structure enables full control of the quantum state, as illustrated by our demon-

stration of coherent transfer to a chosen hyperfine state in either the first-excited or ground rotational state. Such complete control is essential for many proposed applications of ultracold polar molecules, and opens the door to a range of exciting future experimental directions, including studies of quantum magnetism [14, 15] and novel many-body phenomena [5, 40].

ACKNOWLEDGMENTS

This work was supported by the U.K. Engineering and Physical Sciences Research Council (EPSRC) Grants No. EP/H003363/1, EP/I012044/1, and GR/S78339/01. JA acknowledges funding by the Spanish Ministry of Science and Innovation Grants No. CTQ2012-37404-C02, CTQ2015-65033-P, and Consolider Ingenio 2010 CSD2009-00038. The experimental results and analysis presented in this paper are available at DOI:10.15128/r12j62s485j.

-
- [1] S. Ospelkaus, K.-K. Ni, D. Wang, M. H. G. de Miranda, B. Neyenhuis, G. Quémener, P. S. Julienne, J. L. Bohn, D. S. Jin, and J. Ye, *Science* **327**, 853 (2010).
 - [2] R. V. Krems, *PhysChemChemPhys* **10**, 4079 (2008).
 - [3] D. DeMille, *Phys. Rev. Lett.* **88**, 067901 (2002).
 - [4] L. Santos, G. V. Shlyapnikov, P. Zoller, and M. Lewenstein, *Phys. Rev. Lett.* **85**, 1791 (2000).
 - [5] M. A. Baranov, M. Dalmonte, G. Pupillo, and P. Zoller, *Chem. Rev.* **112**, 5012 (2012).
 - [6] V. V. Flambaum and M. G. Kozlov, *Phys. Rev. Lett.* **99**, 150801 (2007).
 - [7] T. A. Isaev, S. Hoekstra, and R. Berger, *Phys. Rev. A* **82**, 052521 (2010).
 - [8] J. J. Hudson, D. M. Kara, I. J. Smallman, B. E. Sauer, M. R. Tarbutt, and E. A. Hinds, *Nature* **473**, 493 (2011).
 - [9] K.-K. Ni, S. Ospelkaus, M. H. G. de Miranda, A. Pe'er, B. Neyenhuis, J. J. Zirbel, S. Kotochigova, P. S. Julienne, D. S. Jin, and J. Ye, *Science* **322**, 231 (2008).
 - [10] T. Takekoshi, L. Reichsöllner, A. Schindewolf, J. M. Hutson, C. R. Le Sueur, O. Dulieu, F. Ferlaino, R. Grimm, and H.-C. Nägerl, *Phys. Rev. Lett.* **113**, 205301 (2014).
 - [11] P. K. Molony, P. D. Gregory, Z. Ji, B. Lu, M. P. Köppinger, C. R. Le Sueur, C. L. Blackley, J. M. Hutson, and S. L. Cornish, *Phys. Rev. Lett.* **113**, 255301 (2014).
 - [12] J. W. Park, S. A. Will, and M. W. Zwierlein, *Phys. Rev. Lett.* **114**, 205302 (2015).
 - [13] M. Guo, B. Zhu, B. Lu, X. Ye, F. Wang, R. Vexiau, N. Bouloufa-Maafa, G. Quémener, O. Dulieu, and D. Wang, *Phys. Rev. Lett.* **116**, 205303 (2016).
 - [14] R. Barnett, D. Petrov, M. Lukin, and E. Demler, *Phys. Rev. Lett.* **96**, 190401 (2006).
 - [15] A. V. Gorshkov, S. R. Manmana, G. Chen, J. Ye, E. Demler, M. D. Lukin, and A. M. Rey, *Phys. Rev. Lett.* **107**, 115301 (2011).
 - [16] K. R. A. Hazzard, A. V. Gorshkov, and A. M. Rey, *Phys. Rev. A* **84**, 033608 (2011).
 - [17] B. Yan, S. A. Moses, B. Gadway, J. P. Covey, K. R. A. Hazzard, A. M. Rey, D. S. Jin, and J. Ye, *Nature* **501**, 521 (2013).
 - [18] A. André, D. DeMille, J. M. Doyle, M. D. Lukin, S. E. Maxwell, P. Rabl, R. J. Schoelkopf, and P. Zoller, *Nature Physics* **2**, 636 (2006).
 - [19] J. W. Park, Z. Z. Yan, L. Huanqian, S. A. Will, and M. W. Zwierlein, *arXiv:1606.04184* (2016).
 - [20] J. Aldegunde, H. Ran, and J. M. Hutson, *Phys. Rev. A* **80**, 043410 (2009).
 - [21] S. Ospelkaus, K.-K. Ni, G. Quémener, B. Neyenhuis, D. Wang, M. H. G. de Miranda, J. L. Bohn, J. Ye, and D. S. Jin, *Phys. Rev. Lett.* **104**, 030402 (2010).
 - [22] B. Neyenhuis, B. Yan, S. A. Moses, J. P. Covey, A. Chotia, A. Petrov, S. Kotochigova, J. Ye, and D. S. Jin, *Phys. Rev. Lett.* **109**, 230403 (2012).
 - [23] S. A. Will, J. W. Park, Z. Z. Yan, H. Loh, and M. W. Zwierlein, *Phys. Rev. Lett.* **116**, 225306 (2016).
 - [24] N. F. Ramsay, *Phys. Rev.* **85**, 60 (1952).
 - [25] J. M. Brown and A. Carrington, *Rotational Spectroscopy of Diatomic Molecules* (Cambridge University Press, Cambridge, U.K., 2003).
 - [26] D. L. Bryce and R. E. Wasylshen, *Acc. Chem. Res.* **36**, 327 (2003).
 - [27] J. Aldegunde, B. A. Rivington, P. S. Żuchowski, and J. M. Hutson, *Phys. Rev. A* **78**, 033434 (2008).
 - [28] H. Ran, J. Aldegunde, and J. M. Hutson, *New J. Phys.* **12**, 043015 (2010).
 - [29] M. L. Harris, P. Tierney, and S. L. Cornish, *J. Phys. B: At. Mol. Opt. Phys.* **41**, 059803 (2008).
 - [30] D. L. Jenkin, D. J. McCarron, M. P. Köppinger, H. W. Cho, S. A. Hopkins, and S. L. Cornish, *Eur. Phys. J. D* **65**, 11 (2011).
 - [31] H. W. Cho, D. J. McCarron, D. L. Jenkin, M. P.

- Köppinger, and S. L. Cornish, *Eur. Phys. J. D* **65**, 125 (2011).
- [32] D. J. McCarron, H. W. Cho, D. L. Jenkin, M. P. Köppinger, and S. L. Cornish, *Phys. Rev. A* **84**, 011603 (2011).
- [33] M. P. Köppinger, D. J. McCarron, D. L. Jenkin, P. K. Molony, H. W. Cho, S. L. Cornish, C. R. Le Sueur, C. L. Blackley, and J. M. Hutson, *Phys. Rev. A* **89**, 033604 (2014).
- [34] P. D. Gregory, P. K. Molony, M. P. Köppinger, A. Kumar, Z. Ji, B. Lu, A. L. Marchant, and S. L. Cornish, *New J. Phys.* **17**, 055006 (2015).
- [35] P. K. Molony, P. D. Gregory, A. Kumar, C. R. Le Sueur, J. M. Hutson, and S. L. Cornish, *Chem. Phys. Chem.* (2016), 10.1002/cphc.201600501.
- [36] C. E. Fellows, R. F. Gutterres, A. P. C. Campos, J. Vergès, and C. Amiot, *J. Mol. Spectrosc.* **197**, 19 (1999).
- [37] P. K. Molony, A. Kumar, P. D. Gregory, R. Kliese, T. Puppe, C. R. Le Sueur, J. Aldegunde, J. M. Hutson, and S. L. Cornish, *Phys. Rev. A* (2016).
- [38] C. W. White, W. M. Hughes, G. S. Hayne, and H. G. Robinson, *Phys. Rev.* **174**, 23 (1968).
- [39] C. W. White, W. M. Hughes, G. S. Hayne, and H. G. Robinson, *Phys. Rev. A* **7**, 1178 (1973).
- [40] L. D. Carr, D. DeMille, R. V. Krems, and J. Ye, *New J. Phys.* **11**, 055049 (2009).